The Muon Front End for the Neutrino Factory

C. T. Rogers
*STFC Rutherford Appleton Laboratory, Harwell Science and Innovation Campus, Didcot. OX11 0QX**

D. Stratakis
Brookhaven National Laboratory, Upton, N.Y. 11973-5000

G. Prior and S. Gilardoni
European Organization for Nuclear Research CERN, CH-1211 Genève 23

D. Neuffer
Fermi National Laboratory, P.O. Box 500, Batavia, IL 60510-5011

P. Snopok
Illinois Institute of Technology, 3300 South Federal Street, Chicago, IL 60647

A. Alekou
Imperial College, London, Imperial College London,
Blackett Laboratory, Prince Consort Rd, London, SW7 2BW

J. Pasternak
Imperial College, London, Imperial College London,
Blackett Laboratory, Prince Consort Rd, London, SW7 2BW and
STFC Rutherford Appleton Laboratory, Harwell Science and Innovation Campus, Didcot. OX11 0QX

In the Neutrino Factory, muons are produced by firing high energy protons onto a target to produce pions. The pions decay to muons and pass through a capture channel known as the muon front end, before acceleration to 12.6 GeV. The muon front end comprises a variable frequency RF system for longitudinal capture and an ionisation cooling channel. In this paper we detail recent improvements in the design of the muon front end.

* chris.rogers@stfc.ac.uk

I. INTRODUCTION

In the Neutrino Factory [1], a 4 MW proton beam is delivered onto a target to create a flux of pions, muons and background particles. The proton beam is delivered in a train of 1-3 bunches produced at 50 Hz. In order for RF cavities in the muon acceleration chain to refill, proton bunches are produced with at least 50 μs intervals.

The Neutrino Factory muon front-end captures secondary particles produced on the target by means of a pion decay channel and particle selection system followed by a longitudinal drift to an adiabatic buncher, energy-phase rotation system, and ionisation cooling channel, after which the beam enters a chain of muon accelerators.

Pions are captured in a solenoidal field that tapers adiabatically from 20 T to 1.5 T while the beam pipe radius increases from 0.075 m to 0.3 m. A large transverse phase space of both positively and negatively charged particles with a large energy spread is captured in the solenoidal field. Protons and other background particles are removed from the beam by means of a bent-solenoid chicane and proton absorber and subsequently a time-energy relationship is allowed to develop.

The beam passes through a series of RF cavities, each of which has frequency selected to be synchronous with particles in the beam and the voltage of each one higher than the previous to adiabatically form microbunches. Once the voltage has reached its nominal peak value, the cavity frequency is chosen so that fast muons at the head of the bunch experience a decelerating phase and slow muons at the tail of the bunch experience an accelerating phase. The phase is chosen so that the head bunch and tail bunch has the same energy when the bunch frequency is 201.25 MHz.

Subsequently the beam enters an ionisation cooling channel. The particles are passed through material absorbers reducing both transverse and longitudinal momentum. They are then reaccelerated in RF cavities replacing momentum in only the longitudinal direction resulting in a reduction of transverse emittance. Multiple Coulomb scattering and energy straggling tend to create noise counteracting the emittance reduction. A low-Z material (Lithium Hydride) is chosen for the absorber to minimise these effects.

In order to maintain a high acceptance, solenoids are tightly packed around RF cavities and absorbers. There are indications that this can facilitate breakdown in the cavities, which may make the baseline parameters challenging to achieve.

Following the muon front end, particles are passed into an acceleration system, accelerated to 12.6 GeV and placed in a storage ring where the majority decay radioactively to form neutrinos. In the baseline, at least 10^{21} muon decays in the production straight are required per year.

The present design is based on the lattice presented in the Neutrino Factory Study 2A report [2] and subsequently developed in the International Scoping Study for a Neutrino Factory (ISS) [3] with several modifications: a particle selection system has been introduced to manage secondaries from the target; the solenoid-field strength in the drift, buncher, and phase rotation sections has been reduced from 1.75 T to 1.5 T; the whole system has been shortened; and the thickness of the Lithium Hydride absorbers in the cooling section has been increased. Additionally a significant effort has been invested in designing alternate schemes for ionisation cooling to mitigate the effect of RF breakdown that may be caused by overlapping magnetic fields with the cavities.

In this paper we summarise these improvements.

II. DECAY REGION AND PARTICLE SELECTION SCHEME

In this study, the input beam to the Neutrino Factory was taken to be composed of a monochromatic 8 GeV proton beam with a 3 ns time spread incident on a liquid Mercury target in the bore of a 20 T solenoid. The interaction of the beam with the target was modelled using the MARS15(2010) default generator [4].

After the target, the field tapers from 20 T to 1.5 T over a distance of 15 m collecting both positive and negative particle species. A large flux of protons of all energies comes off the target up to the energy of incoming protons. Additionally, relatively low energy electrons and pions are produced. The particles pass through a solenoidal chicane where they acquire a vertical dispersion, with oppositely-charged particles gaining a dispersion in the opposite direction. Subsequently particles pass through a Beryllium absorber, which removes almost all of the remaining, low energy, protons.

A. Chicane

The chicane starts 30 m after the proton target. The radius of curvature of the chicane is 22.92 m, with a 12.5° outward bend followed by a 12.5° return bend. This results in a transverse displacement of the decay section by 1.09 m. This prevents the highest energy particles, that are relatively unperturbed by the magnetic field, from passing straight through the chicane. It gives momentum collimation for momenta greater than 500 MeV/c, which

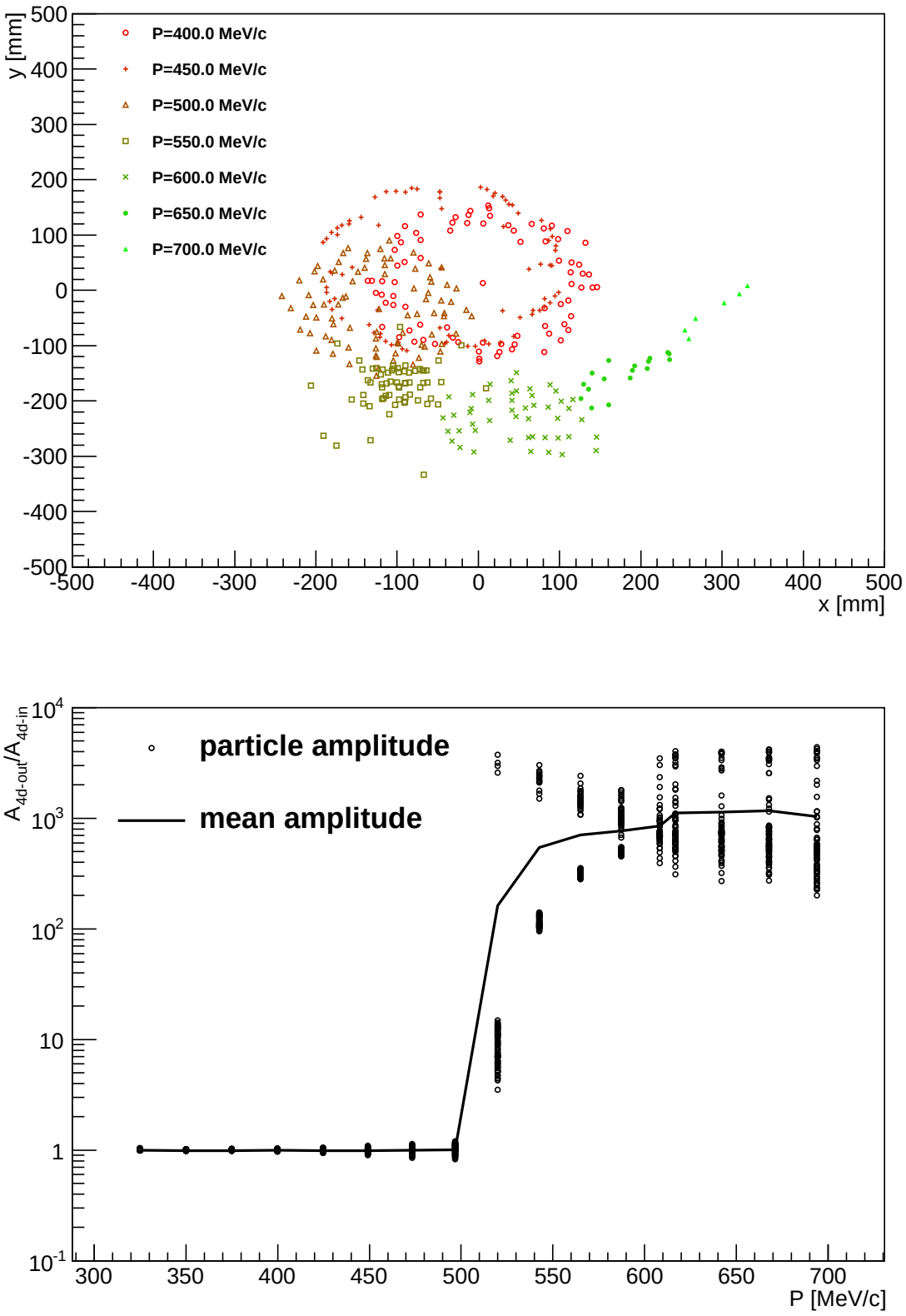

FIG. 1. (top) x-y projection and (bottom) fractional change in transverse amplitude of a shell of muons after transport through the chicane system for a variety of momenta. The muons were created on the surface of a hyperellipsoid in (x, p_x, y, p_y) space at intervals of 25 MeV/c total momentum. The surface was chosen at each momentum to be constant in the 1.5 T field with 4D transverse amplitude of 50 mm. Simulation in MAUS 0.3.1 [5].

is the upper limit for capture by the phase rotation system. By maintaining the symmetry of the chicane, particles within the momentum acceptance are returned to the axis with very little emittance growth.

A simulation of a shell of particles passing through the chicane with initial transverse amplitude of 50 mm is shown in figure 1. The emittance change of particles as a function of momentum is shown together with a projection of the x, y position of the particles after the chicane for a variety of momenta. There is a clear transition at 500–550 MeV/c where particles are no longer transported by the chicane. Below this transition particles are transported with little or no emittance growth, even for a relatively high emittance beam with a very large momentum spread.

B. Proton absorber

Immediately following the chicane a Beryllium absorber is placed in the beam line to remove the remaining proton impurities. Protons with energies in the sub-GeV regime are stopped in considerably less material than lighter particles of the same energy. Stochastic effects can lead to some protons receiving a smaller energy loss and passing through the absorber even for relatively high proton absorber thicknesses. The absorber can also create emittance growth in the muon beam. There is a tension between improving the muon yield with a thinner absorber and decreasing the proton yield with a thicker absorber.

In figure 2 the total proportion of protons and the yield of good muons per proton is shown as a function of chicane bending angle for various absorber thicknesses. There is a good optimum with a bending angle of 12.5° (1.25° per cell) and a proton absorber thickness of 100 mm.

Roughly 0.8 % of the proton beam power (of order 1 kW) remains in the beam. These protons deposit most of their energy in the cooling channel. It is envisaged that a short remote handling section, possibly associated with a pre-cooler, will be necessary around the start of the cooling section to handle these remaining protons.

Beryllium was chosen as a material for the proton absorber as it does not react with water coolants, it is robust to thermal stressing and has low atomic number. In general, low atomic number materials cause less scattering and associated beam heating.

C. Loss Handling

Several 100 kWs of beam power are deposited in the chicane and a significant amount of energy is deposited by showering electrons after the proton absorber. The chicane is comprised mainly of normal conducting coils in order to manage such losses. The electromagnetic shower after the proton absorber is produced mainly by relatively low energy electrons and photons and so direct shielding should be effective in the area downstream of the absorber.

III. IMPROVEMENTS TO THE RF CAPTURE SYSTEM

The RF capture system has been optimised to produce a shortened bunch train by reducing the length of the drift section and other regions. The baseline design delivers a bunch train that is less than 80 m long. This is an improvement over the version of the design developed for the ISS [3] which delivered a 120 m long bunch train containing the same number of muons. A shorter bunch train makes some downstream systems easier to design.

A. Buncher

To determine the required buncher parameters, we consider reference particles (0, N_B) at $p_0 = 233$ MeV/c and $p_{N_B} = 154$ MeV/c, with the intent of capturing muons from an initial kinetic energy range of 50 to 400 MeV. The RF cavity frequency, f_{RF}, and phase are set to place these reference particles at the centre of bunches while the RF voltage increases along the channel. These conditions can be maintained if the RF wavelength, λ_{RF}, increases along the buncher, following:

$$N_B \lambda_{RF}(s) = N_B \frac{c}{f_{RF}(s)} = s \left(\frac{1}{\beta_{N_B}} - \frac{1}{\beta_0} \right) ; \tag{1}$$

where s is the total distance from the target, β_0 and β_{N_B} are the velocities of the reference particles, and N_B is an integer. For the present design, N_B is chosen to be 10, and the buncher length is 33.0 m. With these parameters, the

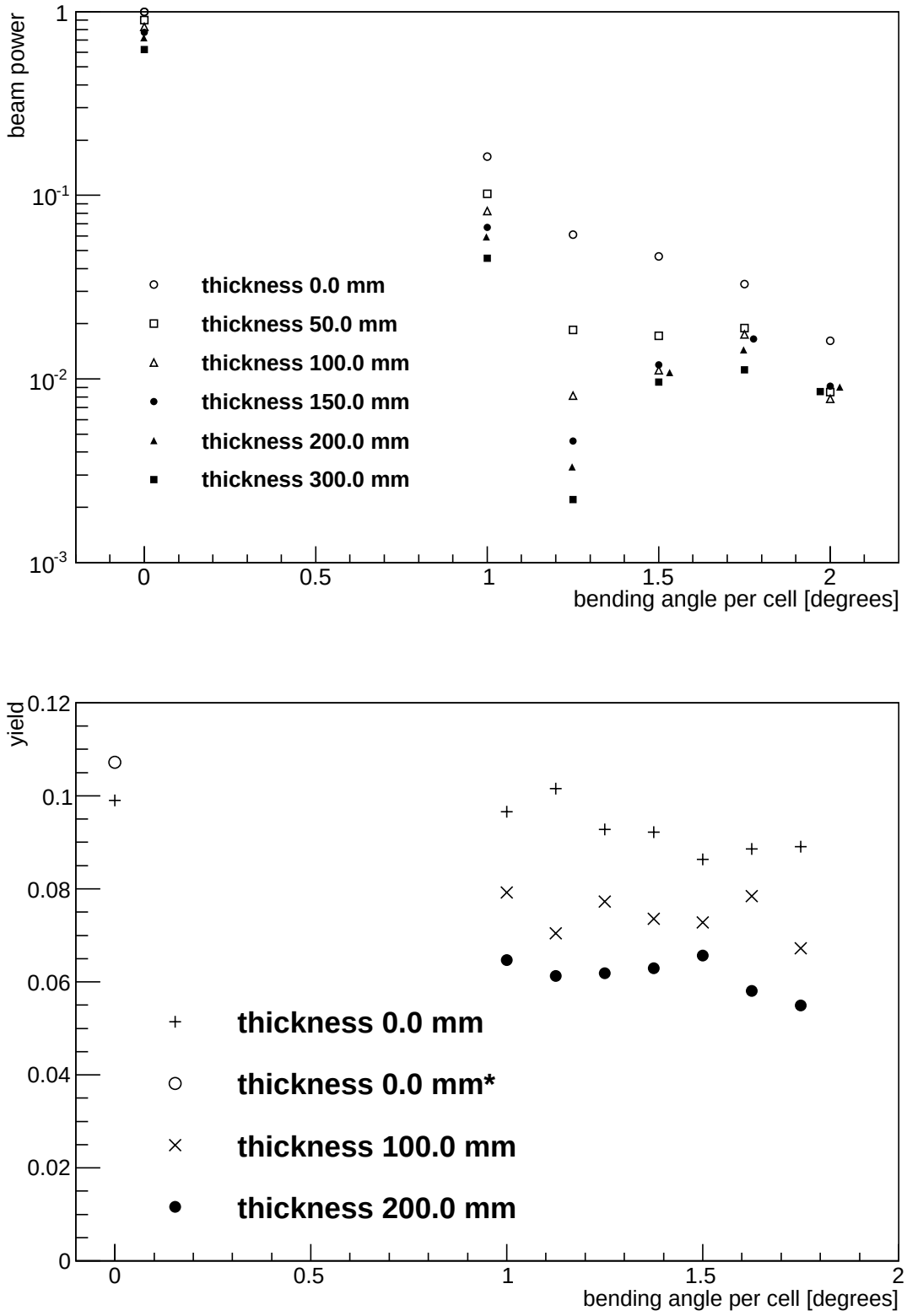

FIG. 2. (top) Fractional power of protons and (bottom) good muon yield at the end of the cooling channel for different chicane bending angles and absorber thicknesses. Overlapping points have been laterally displaced for clarity. The bending angle per cell is shown; each arc of the chicane was simulated with 10 2-coil cells, each of which was rotated in the simulation to provide a smoothly varying solenoid field. No dipole field was applied. A cylindrical Beryllium absorber was placed after the chicane with thicknesses listed. The two points for 0 mm thickness and 0° bending angle in the bottom figure assume (+) ideal constant 1.5 T field and (*) 3D magnetic field maps. All chicane simulations use realistic magnet field maps. Simulation in G4Beamline 2.06 [6].

	Length [m]	Number of cavities	Frequencies [MHz]	Number of frequencies	Peak gradient [MV/m]	Peak power requirements
Buncher	33.0	33	319.6 to 233.6	13	3.42 to 9.01	1–3.5 MW/frequency
Rotator	42.0	56	230.2 to 202.3	15	13	2.5 MW/cavity
Cooler	97.5	130	201.25	1	16	4 MW/cavity
Total	172.5	219	319.6 to 201.25	29		562 MW

TABLE I. Summary of front-end RF requirements. Where power requirement is listed per frequency, this is the requirement per group of RF cavities of the same frequency. Where it is listed per cavity, this is the requirement per single RF cavity. The total installed RF voltage is 1184 MV.

RF cavities decrease in frequency from 320 MHz ($\lambda_{RF} = 0.94$ m) to 230 MHz ($\lambda_{RF} = 1.3$ m) over the length of the buncher.

The initial geometry for the placement of the RF cavities uses $0.4 - 0.5$ m long cavities placed within 0.75 m long cells. The 1.5 T solenoid focusing of the decay region is continued through the buncher and the rotator section which follows. The RF gradient is increased from cell to cell along the buncher, and the beam is captured into a string of bunches, each of which is centred about a test particle position, with energies determined by the spacing from the initial test particle such that the i^{th} reference particle has velocity:

$$1/\beta_i = 1/\beta_0 + \frac{i}{N_B}\left(\frac{1}{\beta_{N_B}} - \frac{1}{\beta_0}\right). \tag{2}$$

In the initial design, the cavity gradients, V_{RF}, follow a linear increase along the buncher:

$$V_{RF}(z) \approx 9\frac{z}{L_B} MV/m\,; \tag{3}$$

where z is distance along the buncher and L_B is the length of the buncher. The gradient at the end of the buncher is 9 MV/m. This gradual increase of the bunching voltage enables a somewhat adiabatic capture of the muons into separated bunches, which minimises phase-space dilution.

In the practical implementation of the buncher concept, this linear ramp of cavity frequency is approximated by a sequence of RF cavities that decrease in frequency along the 33 m beam transport allotted to the buncher. The number of different RF frequencies is limited to a more manageable 13 (1–4 RF cavities per frequency). The linear ramp in gradient described by (3) is approximated by the placement and gradient of the cavities in the buncher. Table I shows a summary of the RF cavities that are needed in the buncher, rotator, and cooling sections.

B. Rotator

In the rotator section, the RF bunch-spacing between the reference particles is shifted away from the integer, N_B, by an increment, δN_B, and phased so that the high-energy reference particle is stationary and the low-energy one is uniformly accelerated to arrive at the same energy as the first reference particle at the end of the rotator. For the baseline, $\delta N_B = 0.05$ and the bunch spacing between the reference particles is $N_B + \delta N_B = 10.05$. This is accomplished using an RF gradient of 13 MV/m in 0.5 m long RF cavities within 0.75 m long cells. The RF frequency decreases from 230.2 MHz to 202.3 MHz along the length of the 42 m long rotator region. A schematic of a rotator cell is shown in figure 3.

The RF frequency is set by requiring that the trajectories of the reference particles be spaced in ct by $(N_B + \delta N_B)$ wavelengths. In a practical implementation, a continuous change in frequency from cavity to cavity is replaced by grouping adjacent sets of cavities into the same RF frequency. The 42 m long RF rotator, then contains 56 RF cavities grouped into 15 frequencies.

Within the rotator, as the reference particles are accelerated to the central energy (at $p = 233$ MeV/c) at the end of the channel, the beam bunches formed before and after the central bunch are decelerated and accelerated respectively, obtaining at the end of the rotator a string of bunches of equal energy for both muon species. At the end of the rotator the RF frequency matches into the RF frequency of the ionisation cooling channel (201.25 MHz). The average momentum at the rotator is 230 MeV/c. The performance of the bunching and phase rotation channel, along with the subsequent cooling channel, is displayed in figure 4, which shows, as a function of the distance down the channel, the number of muons within a reference acceptance. The phase rotation increases the "accepted" muons by a factor of four.

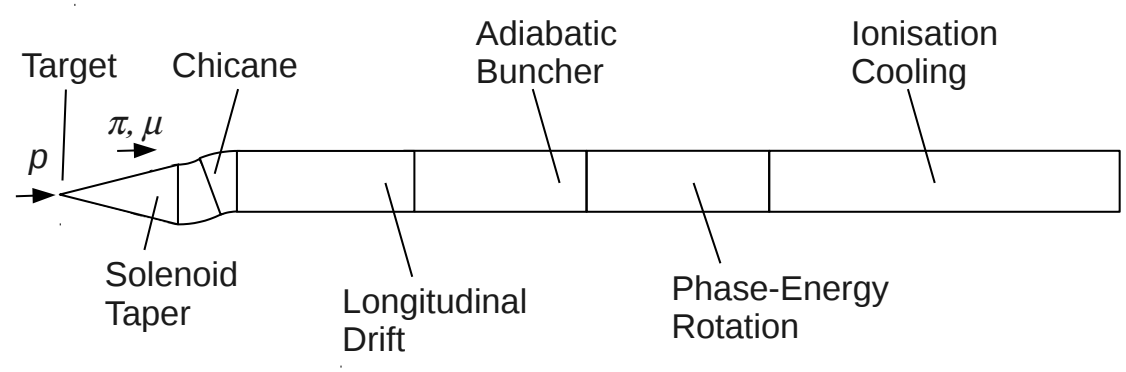

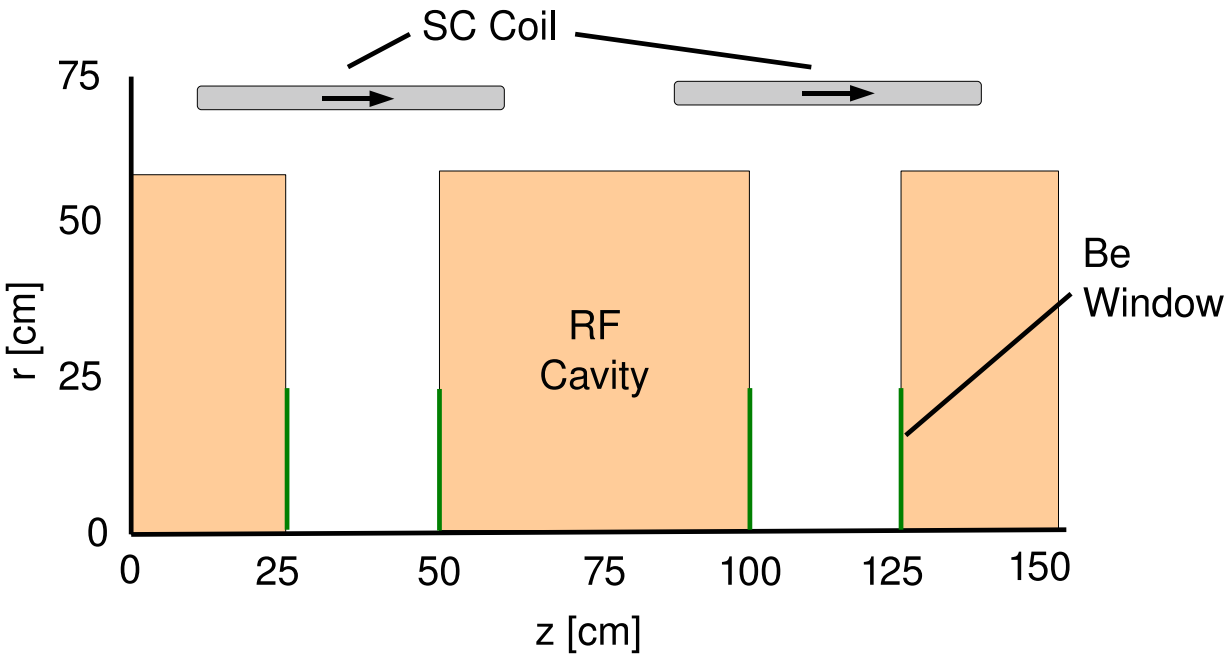

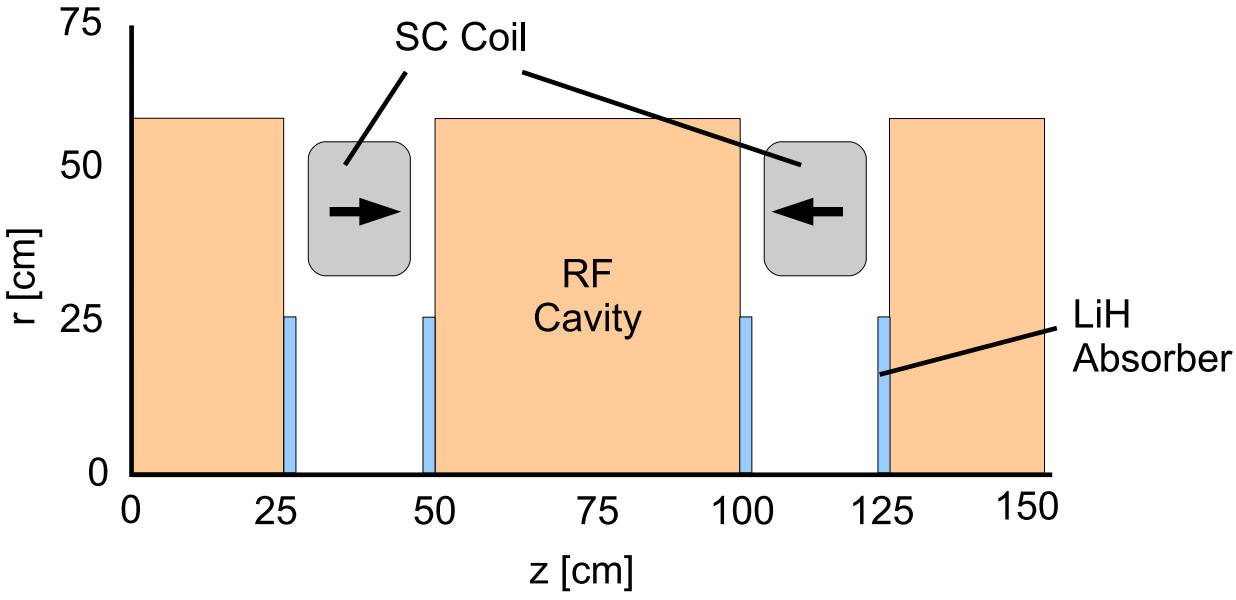

FIG. 3. (top) Schematic of the muon front end, (middle) rotator lattice and (bottom) cooling lattice.

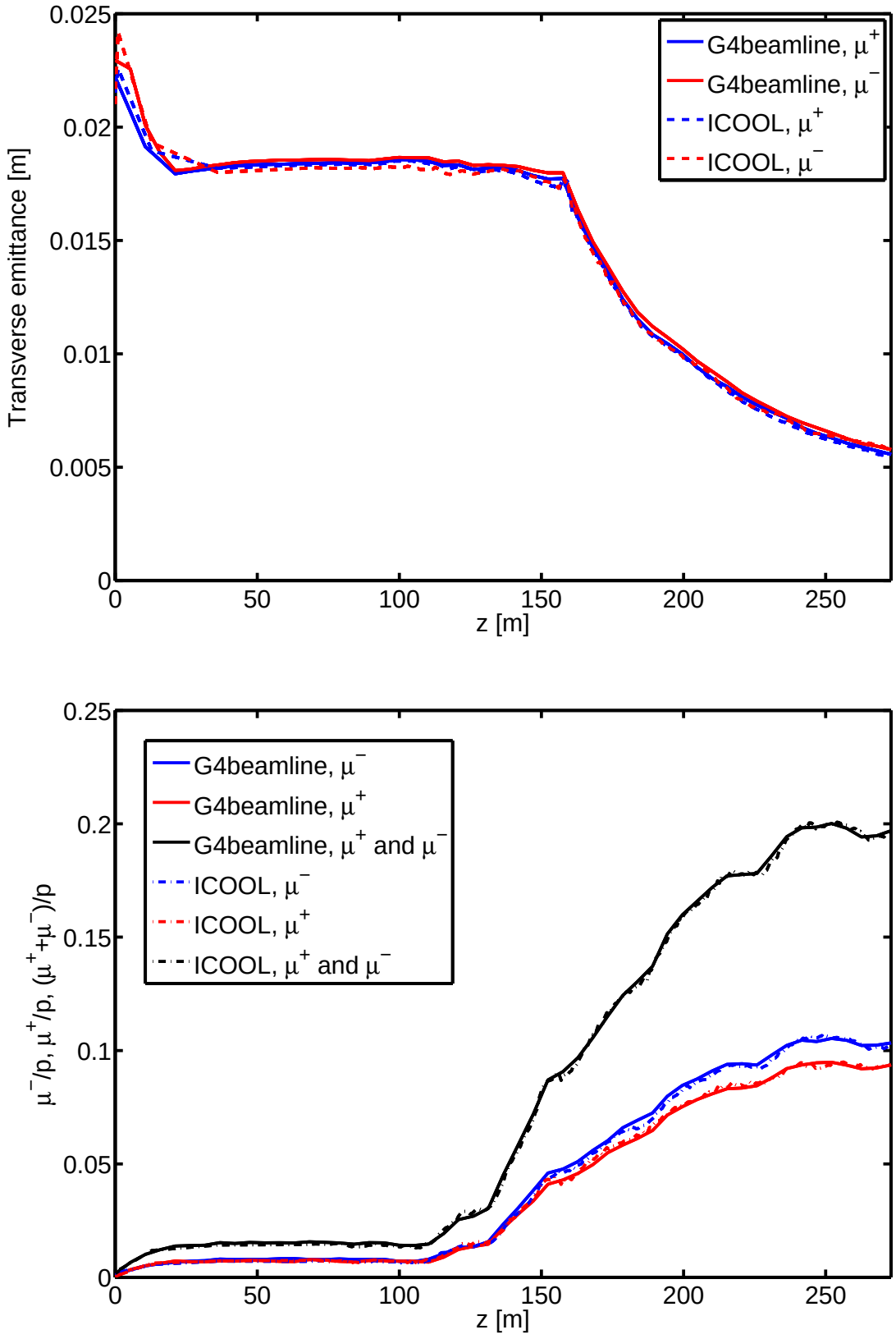

FIG. 4. Performance of the bunching and cooling channel as a function of distance along the channel, as simulated using the ICOOL 3.20 [7] and G4beamline 2.06 [6]. (top) The evolution of the rms transverse emittance (computed over all bunches). (bottom) The evolution of the number of muons within a reference acceptance (muons within 201.25 MHz RF bunches with momentum in the range 100–300 MeV/c, transverse amplitude squared less than 0.03 m and longitudinal amplitude squared less than 0.15 m). The cooling section starts at $s = 155$ m, where the rms transverse emittance is 0.018 m and 0.08 μ per proton are in the reference acceptance. The capture performance is shown for a cooling channel extending to $s = 270$ m although in this design the cooling channel extends only to 230 m. Acceptance is maximal at 0.20 μ per initial 8 GeV proton at $s = 240$ m (85 m of cooling) and the RMS transverse emittance is 7 mm. At $s = 230$ m (75 m of cooling) the number of μs per proton is 0.19 and the transverse emittance is 7.5 mm.

A critical feature of the muon production, collection, bunching, and phase rotation system is that it produces bunches of both signs (μ^+ and μ^-) at roughly equal intensities. This occurs because the focusing systems are solenoids which focus both signs, and the RF systems have stable acceleration for both signs, separated by a phase difference of π. The distribution of muons in longitudinal phase space for particles of both signs at the end of the rotator is shown in figure 5.

IV. IONISATION COOLING CHANNEL

The baseline cooling channel described in [2] remains relatively unchanged. This cooling channel shows a good performance at significant, but probably minimal, cost. The absorber length has been increased by 10 % to take into account modifications to the energy loss in Lithium Hydride in the two main tracking codes used in this study, ICOOL [7] and G4Beamline [6]. It is hoped that these model uncertainties will be resolved by the Muon Ionisation Cooling Experiment (MICE) [8] when it operates in 2014.

The main focus of design effort has been on assessing and mitigating the risk associated with the possibility that the RF cavities specified for the front end and especially the cooling channel may break down in strong magnetic fields reducing the achievable peak field. Development activity has focussed on the cooling channel. While there is a risk of RF breakdown in the buncher and phase rotator, the RF fields and solenoidal fields are lower in here. Additionally, there is no requirement for tight focussing here, unlike in the cooling section, and so it is thought that design of an alternate lattice will be easier.

A. Effect of Reduced RF Gradient

The presence of magnetic fields overlapping RF cavities has been identified as a technical risk that may reduce the capture efficiency of the muon front-end due to a reduction in the peak gradient that can be achieved in the RF cavities [9, 10]. Magnetic insulation of RF cavities [11] [12] and cooling channels filled with insulating high pressure gas have been proposed as a mode to prevent this breakdown [13]. In Europe the focus has been on shielding cavities from RF fields, both by increasing the cell length of the cooling cell [14] and by reducing magnetic fields in the RF cavities using bucking coils [15] [16].

If the RF cavities in the cooling channel fail to reach the desired gradient it can lead to a degradation in muon capture performance. The good muon yield is considered to be the number of muons in a 200 MeV/c momentum bite centred around the reference momentum within a 30 mm transverse amplitude and a 150 mm longitudinal acceptance. This is considered to be the nominal acceptance of the downstream acceleration system.

The degradation in performance of the baseline cooling channel with RF voltage in the cavities is shown in figure 6. The reduction in cooling performance is linear with RF gradient.

B. Bucked Coils

The principle problem in the ionisation cooling channel is to get a tight focus on the emittance absorbers while maintaining a high transverse acceptance. One way to achieve a high acceptance is by tightly packing solenoids, but this leads to overlapping magnetic fields with RF cavities which causes breakdown. The idea of shielding the cavities has been investigated, and yielded some success, but shielding tends to reduce the dynamic aperture of the coils.

The performance of two bucked coil lattices is shown in figure 7. Two lattices are shown, one with shielding provided by bucked coils arranged radially and one with shielding provided by bucked coils arranged laterally. The cavity remains in a field around 1 T, and the good muon yield is reduced by around 15 %. The magnetic field on the cavity is substantially lower, although further experimental guidance is required to confirm that higher gradients can be achieved in such a field.

C. Increased Cell Length

Another way to achieve improved acceptance is to increase the beam energy, taking advantage of the geometrical emittance effect. The RF capture scheme outlined above can capture muons at higher energy by working with a small accelerating phase in the phase rotation section. Operation at higher energy can enable use of a lattice with a reasonable acceptance even with a rather long cell length.

The performance of two lattices with a cell length of 3 m is shown in figure 8. In the first case a liquid Hydrogen absorber is used and the cavity sits in a magnetic field of at worst 1 T. The baseline performance is recovered in this case. In the second case a Lithium Hydride absorber is used. As this material is more dense, and safety windows are not required, the absorber and RF assembly can be made shorter so in this case the cavities sit in at worst a 0.3 T field. The liquid Hydrogen absorber is lower Z and so gives better cooling performance recovering the baseline cooling performance, while the use of Lithium Hydride leads to a worse cooling performance but at lower risk.

The main issue with these lattices is that cooling goes with the fractional decrease in energy. Operation at higher energy requires a larger decrease in energy to get the same emittance reduction, and hence a larger increase in energy i.e. more RF cavities. The ionisation cooling channel comprises a rather large fraction of the total accelerator facility cost and the RF cavities comprise the majority of this expense.

V. SUMMARY

The Neutrino Factory muon front-end captures a substantial proportion of the muons produced by the Neutrino Factory target. Longitudinal capture is achieved using a buncher and energy-time phase-rotation system while transverse capture is achieved using a high field solenoid adiabatically tapered to 1.5 T and enhanced by ionisation cooling.

Technical risks to the muon front-end are presented by the requirement for high peak RF fields in the presence of intense magnetic fields and irradiation of the accelerator hardware due to uncontrolled particle losses. Strategies have been outlined by which these risks can be mitigated. Overall, the muon front-end increases the capture rate of muons in the nominal accelerator acceptance by a factor 10.

VI. ACKNOWLEDGEMENTS

We acknowledge the financial support of the European Community under the European Commission Framework Programme 7 Design Study: EUROnu, Project Number 212372. The EC is not liable for any use that may be made of the information contained herein. We also thank colleagues from the International Design Study (IDS-NF) collaboration for fruitful discussions concerning this work.

[1] S. Choubey et al. International design study for the neutrino factory : Interim design report. Technical Report RAL-TR-2011-018, Rutherford Appleton Laboratory, 2011.

[2] C. Albright et al. The neutrino factory and beta beam experiments and development. 2004.

[3] M. Apollonio et al. Accelerator Design Concept for Future Neutrino Factories. *JINST*, 4:P07001, 2009.

[4] N.V. Mokhov. Recent MARS15 developments: Nuclide Inventory, DPA and Gas Production. Technical Report Fermilab-Conf-10-518-APC, Fermi National Laboratory, 2010.

[5] C. Tunnell and C. T. Rogers. Maus: Mice analysis user software. In *Proceedings of IPAC'11, San Sebastian, Spain*, 2011.

[6] T. J. Roberts et al. G4Beamline particle tracking in matter-dominated beam lines. In *Proceedings of EPAC08, Genoa, Italy*. EPAC, European Physical Society Accelerator Group, 2008.

[7] R. C. Fernow. Recent developments on the muon-facility design-code ICOOL. In *Proceedings of 2005 Particle Accelerator Conference, Knoxville, Tennessee*, pages 2651–2653, Piscataway, NJ, 2005. IEEE.

[8] A. Blondel. The mice experiment. In *Proceedings of IPAC'12, New Orleans, USA*, 2012.

[9] A. Moretti et al. Effects of high solenoidal magnetic fields on rf accelerating cavities. *Phys. Rev. ST Accel. Beams*, 8:072001, 2005.

[10] R. B. Palmer et al. RF breakdown with external magnetic fields in 201 and 805 MHz cavities. *Phys. Rev. ST Accel. Beams*, 12:031002, 2009.

[11] J. C. Gallardo D. Stratakis and R. B. Palmer. Magnetically insulated high-gradient accelerating structures for muon acceleration. *J. Phys. G*, 37:105011, 2010.

[12] D. Stratakis et al. Numerical study of a magnetically insulated front-end channel for a neutrino factory. *Phys. Rev. ST Accel. Beams*, 14:011001, 2011.

[13] J. C. Gallardo and M. S. Zisman. A possible hybrid cooling channel for a neutrino factory. In *Proceedings of IPAC'10, Kyoto, Japan*, pages 3515–3517. IPAC'10 and Asian Committee for Future Accelerators, 2010.

[14] C. T. Rogers. Design for a Muon Front End with Magnetically Shielded RF Cavities. In Maury C. Goodman, Daniel M. Kaplan, and Zach Sullivan, editors, *Neutrino Factories, Superbeams and Beta Beams: 11th International Workshop on Neutrino Factories, Superbeams and Beta Beams—NuFact09*, volume 1222 of *AIP Conference Proceedings*, pages 298–302, Melville, NY, 2010. American Institute of Physics.

[15] A. Alekou. *Ionisation cooling lattices for the Neutrino Factory.* PhD thesis, Imperial College, London, 2012.

[16] A. Alekou and J. Pasternak. Bucked coils lattice: A novel ionisation cooling lattice for the neutrino factory. *Journal of Instrumentation*, page 08017, 2012.

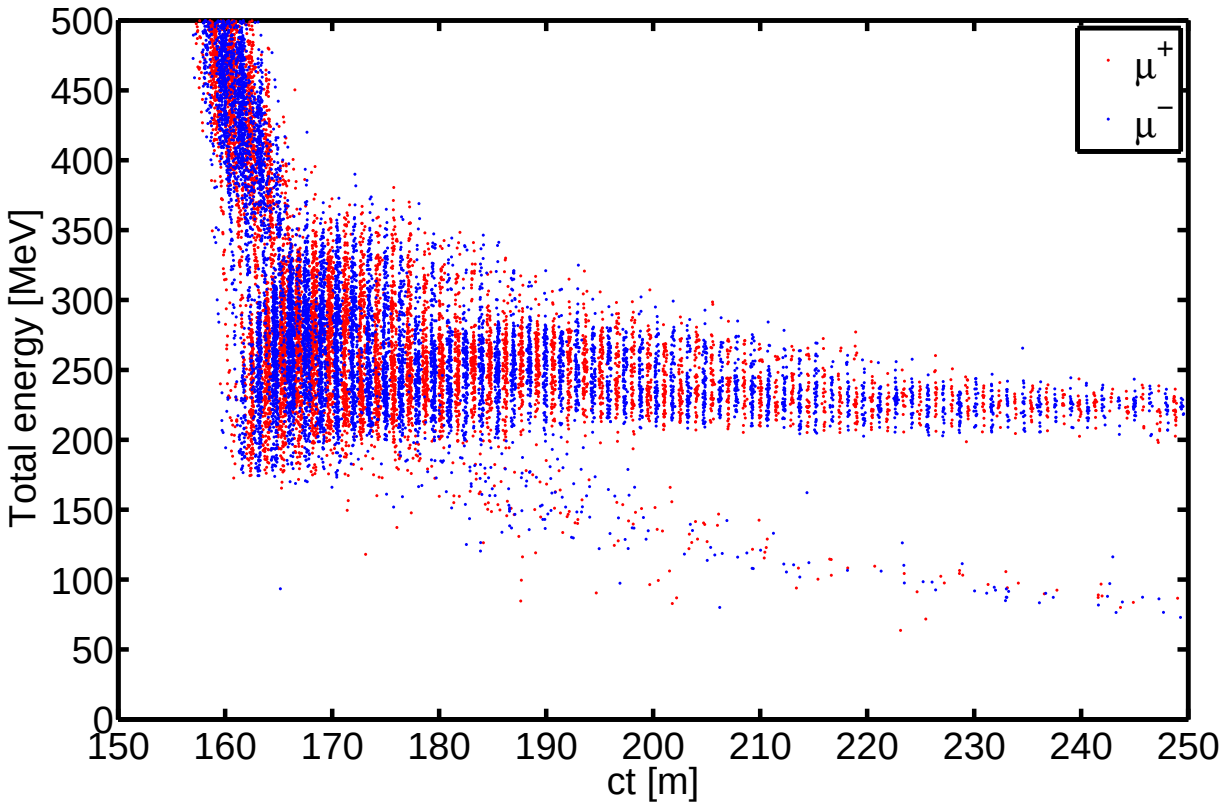

FIG. 5. Distribution of particles in longitudinal phase-space at the phase rotation end. $\mu+$ are shown in red and $\mu-$ are shown in blue.

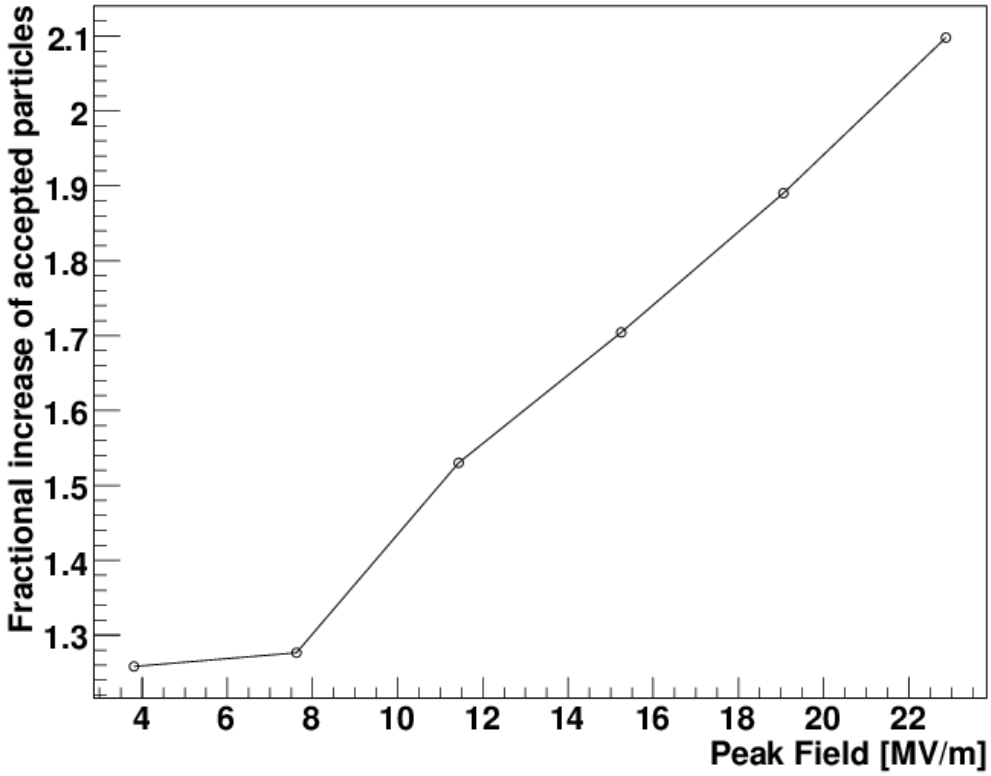

FIG. 6. The degradation in cooling performance with decreased RF voltage is shown. The baseline cooling lattice was simulated with Lithium Hydride thickness proportional to RF peak voltage to account for the reduction in energy gain and the number of muons within the accelerator acceptance was calculated before and after the cooling channel. The ratio of these two values was plotted against cooling channel RF field for a number of peak fields. The nominal cooling channel RF voltage is 16 MV/m.

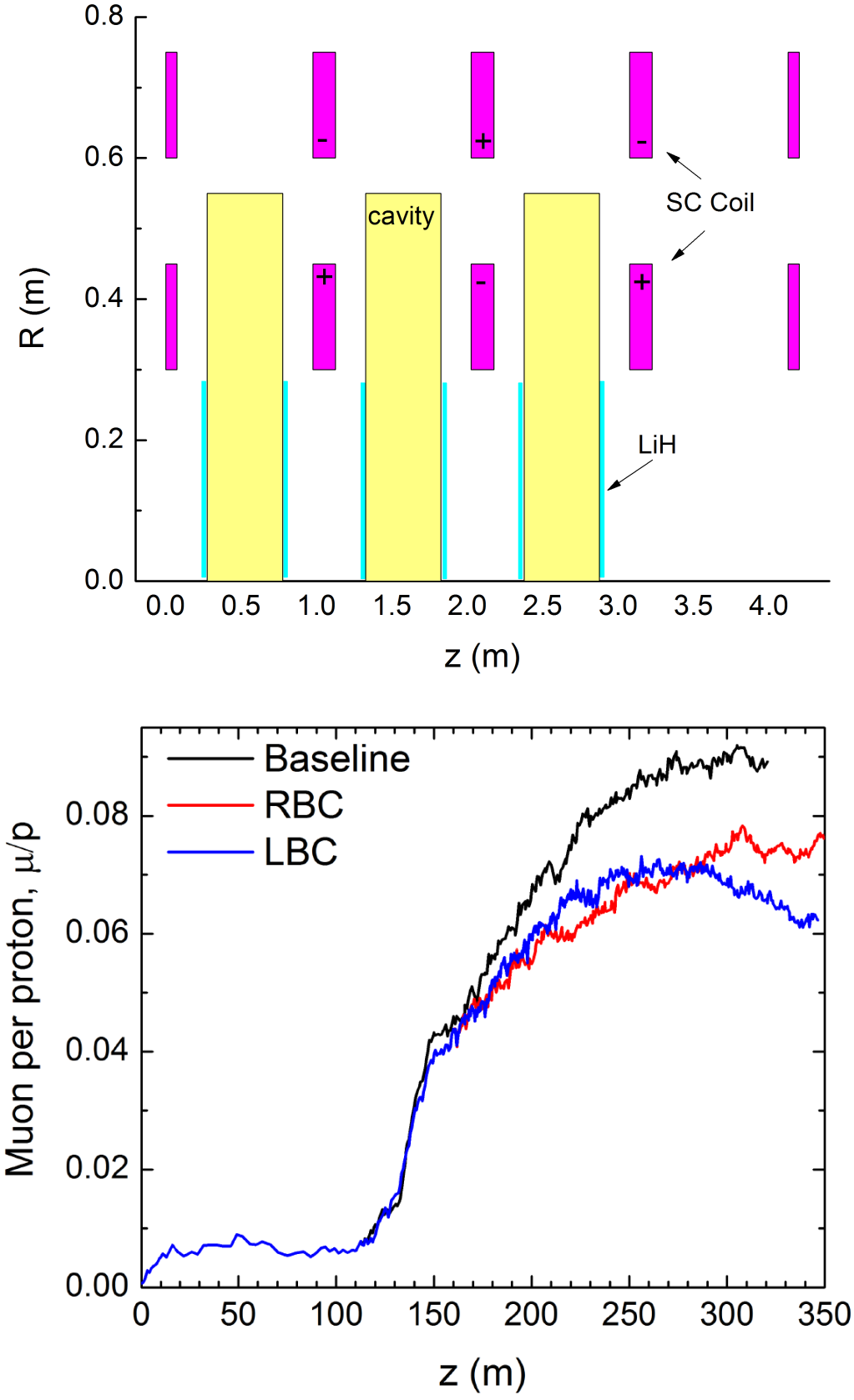

FIG. 7. Schematic of a bucked coil lattice in radially bucked coil (RBC) arrangement and simulated good muon yield with radially bucked coil and laterally bucked coil (LBC) lattices. The bucked coils were used also in the phase rotation section in these simulations.

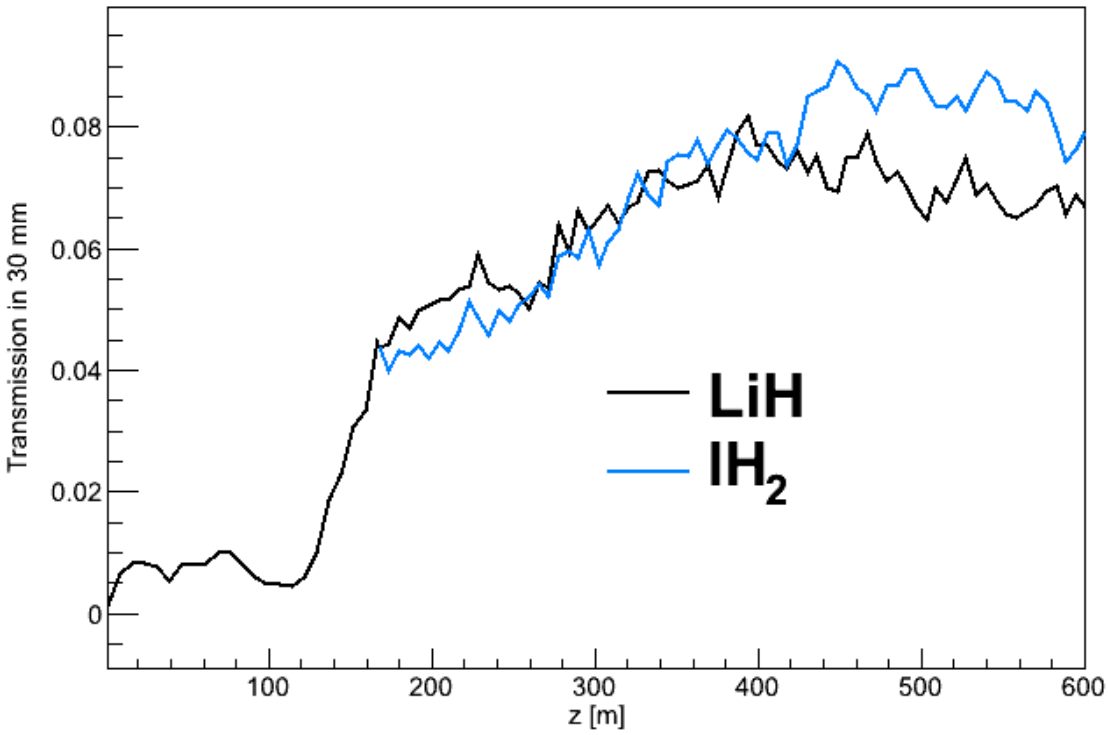

FIG. 8. Simulated good muon yield of $\mu+$ with capture optimised for higher energy and a cooling cell length of 3 m as opposed to 0.75 m in the baseline. The RF capture scheme was adjusted to capture at a central momentum of 273 MeV/c rather than the nominal 214 MeV/c of the baseline lattice. Two absorber materials were simulated, Lithium Hydride (LiH) and liquid Hydrogen (lH_2).